SCIENCE CHINA
Information Sciences

• RESEARCH PAPERS •

September 2011 Vol. 54 No. 9: 1945–1956
doi: 10.1007/s11432-011-4264-1

Experimental investigation of MIMO relay channels statistics and capacity based on wideband outdoor measurements at 2.35 GHz

NIE Xin[1,2*], ZHANG JianHua[1,2], LIU ZeMin[1] & ZHANG Ping[1,2]

[1]*Key Laboratory of Universal Wireless Communications, Ministry of Education; Beijing University of Posts and Telecommunications, Beijing* 100876*, China;*
[2]*Wireless Technology Innovation Institute, Beijing University of Posts and Telecommunications, Beijing* 100876*, China*

Received May 15, 2009; accepted February 5, 2010; published online May 31, 2011

Abstract Relay, which serves to enhance the performance of future communication networks, is one of the most promising techniques for IMT-Advanced systems. The potential performance improvement of relay is investigated in this work. Our investigation consists of two steps. In the first step, to obtain a better understanding of the fundamental properties of relay channels, we conducted outdoor measurements at 2.35 GHz with 50 MHz bandwidth in a typical urban area of China. Three links constituting the relay transmission, i.e., the link between base station and relay station, the link between relay station and mobile station and the link between base station and mobile station were measured by employing a real-time channel sounder. Two main factors that affect the MIMO channel capacity, i.e., the channel gain and effective degrees of freedom, are investigated. The cross-polarization discrimination was obtained by utilizing space-alternating generalized expectation-maximization algorithm. The channel parameters of the three links are statistically analyzed and compared. In the second step, based on the measured data, the performance of different relaying schemes, i.e., amplify-and-forward and decode-and-forward, is evaluated. The impact of RS antenna configuration on the capacity is also analyzed. The measurement and evaluation results reveal that the relay can significantly improve the system coverage and performance.

Keywords MIMO relay channels, IMT-Advanced frequency band, channel characteristics, relay performance evaluation

Citation Nie X, Zhang J H, Liu Z M, et al. Experimental investigation of MIMO relay channels statistics and capacity based on wideband outdoor measurements at 2.35 GHz. Sci China Inf Sci, 2011, 54: 1945–1956, doi: 10.1007/s11432-011-4264-1

1 Introduction

With the gradual success of the 3rd generation mobile communication technology, the research and development of the IMT-Advanced mobile communication have been initiated worldwide. The frequency band from 2.3 to 2.4 GHz was allocated for the IMT-Advanced systems by the World Radiocommunication Conference in 2007. To meet the technical requirements of the IMT-Advanced system, the room for system performance enhancement would be in the area of radio network, with some new techniques probably to

*Corresponding author (email: niexin1983@gmail.com)

be introduced. The relay-based technique is regarded as one of the most promising candidate techniques for IMT-Advanced systems, and has been attracting much attention because of its various advantages over conventional cellular systems regarding the enhancement of diversity, achievable rates and coverage range [1, 2]. The relay-based multiple-input multiple-output (MIMO) system is typically comprised of the base station (BS), the relay station (RS), and the mobile station (MS), each equipped with multiple antennas. The RS forwards the data received wirelessly from the BS to the MS, and vice versa. Thus, the relay channel consists of three links, namely the link between the BS and the RS (BS-RS), the link between the RS and the MS (RS-MS), and the link between the BS and the MS (BS-MS). Amplify-and-forward (AF) and decode-and-forward (DF) are two typical relaying schemes.

The theoretical performance of relay-based MIMO system has been analyzed in many papers [3, 4]. However, most of existing researches on relay-based systems have been carried out under simplified assumption for the channel properties. For example, the Rayleigh channel, which no longer holds when the line-of-sight (LOS) propagation exists, is widely used for analysis [5, 6]. Thus, more details need to be included in the channel model for a more accurate performance evaluation of relay-based systems. To obtain a more thorough understanding of the fundamental properties of relay channels, relay channel measurements and impact of propagation channels on the system performance are discussed by several researchers lately. In [7, 8], the rate improvement by utilizing relay has been investigated and the performance of different relaying schemes is assessed under real indoor propagation channel. The effect of relay location on channel rank has been reported in [9]. The achievable performance of relay system in real outdoor-to-indoor scenario is predicted in [10]. However, due to the limitation of experimental facilities, the propagation statistics of relay channels are left undiscussed in former works. Little attention is paid to the different channel characteristics of three links composing relay channel. Moreover, the measurement and analysis results of wideband outdoor relay channel are scarce. Most former measurements were conducted in indoor [7, 8] or outdoor-to-indoor scenarios [10]. Besides, none of these measurements was conducted in frequency bands allocated to the IMT-Advanced system. Finally and most importantly, due to the variation in layout of buildings, building materials, user density, the propagation environments in China manifest different characteristics from environments in Europe. Our former measurement results in the conventional BS-MS link indicate that the divergence in the statistics of channel parameters is significant, no matter whether in indoor [11] or outdoor [12] scenarios. Thus, an insight into the characteristics of relay channel in typical propagation environments of China is of important significance for the deployment of relay-based communication systems in China.

In order to investigate the characteristics of outdoor relay channels, we conducted a measurement campaign at the center frequency of 2.35 GHz with 50 MHz bandwidth in a typical urban area of China. To the best of our knowledge, this is the first MIMO relay measurement conducted in China. The channel sounding for relay measurement consists of measurements of three individual links, i.e., the BS-MS link, the BS-RS link and the RS-MS link. Our contributions in this paper are threefold. First of all, the different properties in three links of relay channel are obtained. Due to the antenna height of the RS, the channels of BS-RS and RS-MS link manifest different characteristics from conventional link BS-MS. Two main factors that affect the MIMO channel capacity, i.e., the channel gain (CG) and effective degrees of freedom (EDOF), are investigated. The cross-polarization discrimination (XPD), which has great impact on polarization diversity, is also studied. Next, the performance of a variety of transmission schemes based on measured channel is evaluated. The capacity results as a function of the distance to the BS in both LOS and non-line-of-sight (NLOS) scenarios are presented. The evaluation based on measured channels takes into account more factors of the real propagation environment, and is expected to be more accurate. Finally, the impact of antenna configuration on the relay performance is discussed. The effect of spatial correlation and polarization correlation in different propagation environments are analyzed. The measurement and analysis results given in this paper are informative to provide guidelines for relay-based system deployment. The achievement of the different statistics of the relay channel from the conventional channel can also provide important basis for the future relay channel modeling.

The rest of this paper is organized as follows. Section 2 describes the measurement equipments and environment. Section 3 shows the procedure of data post-processing. Section 4 presents the results of

Table 1 Measurement parameters

Items	Settings	Items	Settings
Carrier frequency (GHz)	2.35	Number of RS antenna N_{RS}	8
Bandwidth (MHz)	50	Number of MS antenna N_{MS}	8
Code length (chips)	255	Height of BS antenna (m)	22
Transmitting power (dBm)	26	Height of RS antenna (m)	7
Types of antennas	ODA	Height of MS antenna (m)	1.8
Number of BS antenna N_{BS}	8		

the measurement including CG, EDOF, and XPD. Section 5 evaluates the capacity of different transmitting schemes. The impact of antenna configuration on capacity is also analyzed. Section 6 gives the conclusion of our work.

2 Measurement

2.1 Equipment

The Elektrobit PropSound Channel Sounder was employed. The sounder works in a time-division multiplexing (TDM) mode. Periodic pseudo random binary signals (PRBS) are transmitted between different sub-channels. The interval within which all sub-channels are sounded once is referred to as a measurement cycle[1)]. The 28-element cylinderal omni-directional array (ODA) was utilized at BS, RS and MS. Every element of the ODA consists of two co-located dual-polarized patches, the polarization directions of which are $+45^\circ$ and -45° with respect to the vertical, respectively. The spacing between the neighboring elements is half a wavelength. One ring of the elements was selected as the active antenna, i.e., 8 dual-polarized patch elements. The antenna pattern was obtained from Satimo SG128 antenna measurement system. The measurement settings are summarized in Table 1.

2.2 Environment

The measurement was carried out in a typical urban area of Beijing, China. The measurement scenario is illustrated in Figure 1. The measurement area is characterized by buildings ranging from 4 to 8 floors. The BS antennas were placed on the roof top of a 5-floor building, which was about 22 m in height. Considering the height of the relay antenna did not need to be as high as the BS in order to reduce operating and maintenance costs [2], the RS antennas were placed on a testing vehicle around 7 m above the street. In addition, there was typically the LOS between BS and RS to maximize the coverage [13], so the RS was placed in the LOS area of BS. The horizontal distance between the BS and the RS was 107 m. The MS antennas were mounted on a trolley. The height of the MS antennas was adjusted to about 1.8 m in order to imitate the height of human body. By moving the MS antennas, eight continuous routes were measured. The positions of MS were recorded by Global Positioning System. The description for propagation condition of every route in BS-MS and RS-MS link is given in Table 2. Both LOS and NLOS scenarios are measured.

2.3 Phase noise mitigation

The channel sounder working in the TDM mode suffers the phase noise (PN) of local oscillators at the transmitter (Tx) and receiver (Rx) unit, which leads to the overestimation of the channel capacity [14]. The PN is caused by the jitter of local oscillators, and cannot be eliminated completely. Three methods were adopted to reduce the impact of the PN. Firstly, the synchronization between Tx and Rx unit of the sounder was conducted every one hour to weaken the long-term PN [15]. Secondly, using larger number of antennas can mitigate the PN to some extent [16]. Thus, we employed 8 Tx and 8 Rx antennas when

1) More details about the sounder can be found in http://www.electrobit.com/index.php?209.

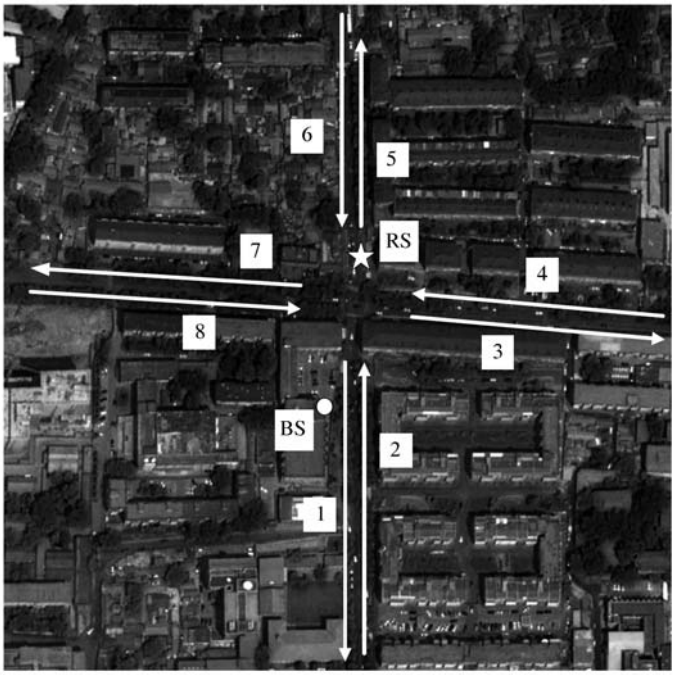

Figure 1 Vertical view of measurement scenario. The circle mark indicates the position of the BS, while the star mark indicates the position of the RS. The straight links with arrow denote routes of the MS, and the arrow indicates the movement direction of the MS.

Table 2 Description for propagation condition for MS routes

Route	BS-MS	RS-MS
1–2	LOS	LOS
3–4	NLOS	NLOS
5–6	NLOS	LOS
7–8	NLOS	NLOS

conducting the measurement. Finally, the non-separable spatial-time array [17] of the sounder can alleviate the impact of the PN. Therefore, the spatial-time array of the sounder was set to be non-separable during the measurement.

3 Data post-processing

Raw data collected by the Rx of channel sounder were the spread signals with the system impulse response of the sounding system. In order to remove the effect of the sounding system, raw data were cyclically correlated with the system impulse response, which was obtained from the calibration of the sounder. Then, channel impulse responses (CIRs), i.e., $h(t,\tau)$, were calculated through the cyclic correlation with the known PRBS. Since the noise level P_n varies with time, the noise level estimation was done for each measurement cycle. To ensure that the signal is much stronger than the noise so that the additive noise does not affect the inherent characteristic of the channel, a threshold P_t was then determined by both the estimated noise level P_n and the peak power of CIRs P_p,

$$P_t = \max\{P_n + D_m, P_p - D_r\}, \tag{1}$$

where D_m is the noise margin from noise floor P_n, and D_r denotes the dynamic range from the peak power P_p. Paths with power $|h(t,\tau)|^2$ below the threshold level P_t were ignored. The dynamic range D_r was set at 25 dB and the margin D_m was set at 6 dB. After the noise-cut, the corresponding frequency

transfer functions $\boldsymbol{H}(t,f)$ can be obtained via the Fourier transform. Assuming that the $\boldsymbol{H}(j,k)$ is the sample of $\boldsymbol{H}(t,f)$, we get

$$\boldsymbol{H}(j,k) = \boldsymbol{H}(t,f)|_{t=j\cdot\Delta t, f=k\cdot\Delta f} = \boldsymbol{H}(j\cdot\Delta t, k\cdot\Delta f), \tag{2}$$

where Δt and Δf are the sampling intervals in the time and frequency domain, respectively. $\boldsymbol{H}(j,k)$ is an $N_{\mathrm{Rx}} \times N_{\mathrm{Tx}}$ matrix with N_{Tx} and N_{Rx} denoting the antenna number of Tx and Rx of the link, respectively.

Channel parameter estimation. Space-alternating generalized expectation-maximization (SAGE) [18], which is well suited for MIMO channel parameter estimation, is used to extract the channel parameters. SAGE is based on the maximum likelihood method and allows for joint estimation of the polarization matrix $\boldsymbol{A}$ of the ℓth multipath component (MPC) from the CIR. The $\boldsymbol{A}_\ell$ reads

$$\boldsymbol{A}_\ell \doteq \begin{bmatrix} \alpha_{\ell,V,V} & \alpha_{\ell,V,H} \\ \alpha_{\ell,H,V} & \alpha_{\ell,H,H} \end{bmatrix}. \tag{3}$$

The entry $\alpha_{\ell,p,q}, p \in \{V,H\}, q \in \{V,H\}$ is the complex gain of q-to-p polarization of the MPC. In order to extract all dominant paths to exactly characterize the propagation environment, 30 MPCs with strongest power were estimated in each measurement cycle.

4 Measurement results and analysis

4.1 Channel gain

With the same transmitting power, the signal-to-noise ratio (SNR) at the Rx is determined by the CG. The effect of slow fading is removed by taking the sliding mean of the sequence of the measured channel transfer matrices (CTMs) by

$$\|\boldsymbol{H}^{avr}(j,k)\|_F^2 = \frac{1}{2N_{sw}+1}\sum_{j-N_{sw}}^{j+N_{sw}} \|\boldsymbol{H}(j,k)\|_F^2, \tag{4}$$

where the superscript *avr* refers to the sliding mean. The length of the sliding window is $2N_{sw}+1$. The N_{sw} is selected having the value of 100 such that the measured CTMs in one sliding window are in a local area, the radius of which is 20 times of the wavelength. After the sliding mean operation, the CG can be calculated from the averaged CTMs as

$$CG(j) = 10\cdot\log_{10}\left(\frac{1}{K}\sum_{k=1}^{K}\|\boldsymbol{H}^{avr}(j,k)\|_F^2\right), \tag{5}$$

where K is the number of frequency bins of jth time realization, and $\|\cdot\|_F$ denotes the Frobenius-norm.

Using eqs. (4) and (5) , the channel gain of all three links can be obtained. The average CG of BS-RS link is -64.6 dB. For both BS-MS and RS-MS links, the CG of all measurement routes as a function of MS position are shown in Figure 2. Colors represent CG in dB. The numbers of routes are shown in Figure 1. The position of RS is the origin of the 2D-Cartesian coordinate system. We observe from Figure 2(a) that the BS provides a better coverage for the route nearby, i.e., routes 1 and 2. The CG of routes 5 and 6 is higher than other routes in the NLOS area, which is mainly due to the waveguide effect of street canyon. It can be seen from Figure 2(b) that the RS improves the coverage in the northern part of the measurement region, especially in routes 3, 4, 7 and 8. As a result of the increased CG, the SNR in these routes can be improved by 10 to 15 dB with the same transmitting power.

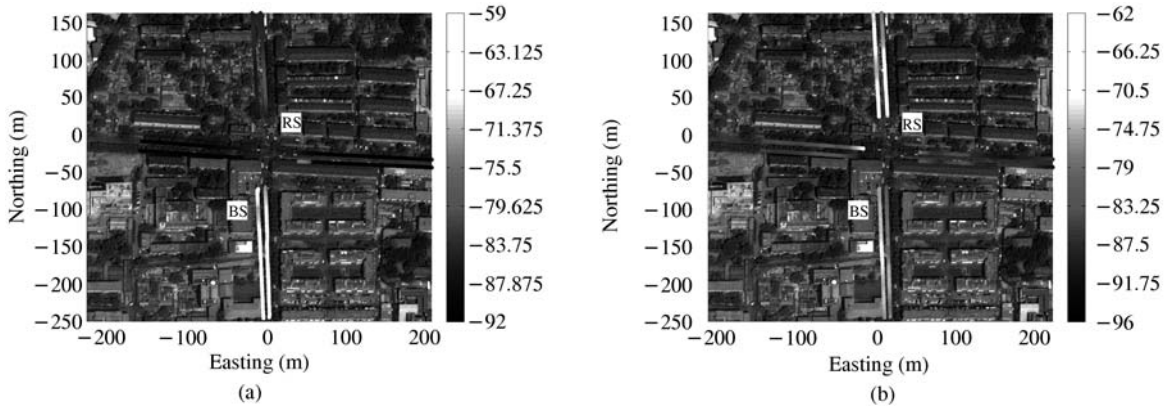

Figure 2 Average channel gain for different routes. (a) Average channel gain of BS-MS link; (b) average channel gain of RS-MS link.

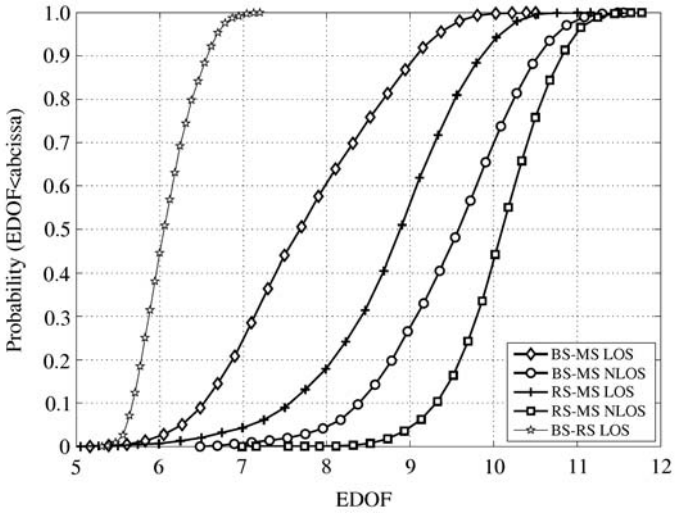

Figure 3 EDOF of different links for both LOS and NLOS cases.

4.2 Effective degrees of freedom

EDOF quantifies the equivalent single-input single-output channels that effectively exhibit channel capacity increases [19]. The EDOF can be obtained as

$$\text{EDOF} = \frac{\partial}{\partial\delta} C(2^{\delta}\rho)\big|_{\delta=0} \tag{6}$$

$$= \frac{\partial}{\partial\delta}\left\{\sum_{r=1}^{R}\log_2\left(1+\frac{2^{\delta}\rho}{N_{\text{Tx}}}\lambda_r\right)\right\}\Big|_{\delta=0} \tag{7}$$

$$= \sum_{r=1}^{R}\frac{\lambda_r\rho}{\lambda_r\rho+N_{\text{Tx}}}, \tag{8}$$

where $\{\lambda_r, r=1,\ldots,R\}$ denote the eigenvalues of $\boldsymbol{H}\boldsymbol{H}^{\text{H}}$, and ρ is the SNR. The richness of the scatters has a significant impact on the EDOF. A channel with rich scatters tends to exhibit high EDOF. The EDOF values of three links when ρ equals 15 dB are plotted in Figure 3.

The mean values of EDOF in the BS-RS, BS-MS and RS-MS link in the LOS scenario are 6, 7, and 8, respectively. It can be concluded that as the height of antennas decreases, the EDOF increases due to richer scatters. It can also be found that the channels in the NLOS scenario exhibit higher EDOF. The mean EDOF of BS-MS and RS-MS link in the NLOS scenario are 8 and 10. Cross-polarized antennas

provide polarization diversity gain in addition to the spatial diversity gain, thus reducing the difference between EDOF in the LOS scenario and that in the NLOS scenario.

4.3 Cross-polarization discrimination

XPD has important influence on the diversity gain. XPD is defined as the co-polarized received signal power to the cross-polarized received power, which is given by

$$\mathrm{XPD}_V = 10 \cdot \log_{10}\left(\left|\frac{\alpha_{V,V}}{\alpha_{H,V}}\right|^2\right)(\mathrm{dB}), \tag{9}$$

$$\mathrm{XPD}_H = 10 \cdot \log_{10}\left(\left|\frac{\alpha_{H,H}}{\alpha_{V,H}}\right|^2\right)(\mathrm{dB}). \tag{10}$$

There is a general consensus in the literature that the XPD, when expressed in dB, has a non-zero-mean Gaussian distribution [20]. Hence we can model the distribution of the XPD as XPD $\sim \mathcal{N}(\mu, \sigma^2)$. The mean value μ and standard deviation σ of the XPD are obtained by utilizing least square fitting. The μ and σ of XPD_V for BS-RS link are 8.0 and 8.0 dB, and meanwhile, the μ and σ of XPD_H for BS-RS link are 6.0 and 9.0 dB. The Gaussian fitting results on BS-MS and RS-MS links are given in Table 4.

The XPD values for BS-RS link are high, indicating little cross-coupling between the orthogonal states of polarization. It can be found from Table 4 that except XPD_V in the NLOS scenario, the XPDs of BS-MS link are larger than those of RS-MS link. The main reason is that due to the lower RS antennas, the increased scatters result in a greater degree of depolarization. We also observe that the XPD_V and XPD_H are almost the same in the LOS scenario. However, in the NLOS scenario, there is a big difference between XPD_V and XPD_H. For the RS-MS link, the difference becomes more remarkable. The results indicate that the vertical polarization preserves better than the horizontal polarization during the propagation, especially in the RS-MS link where the RS antennas are relatively low.

5 Capacity evaluation based on measured channels

Based on $\boldsymbol{H}_0$, $\boldsymbol{H}_1$ and $\boldsymbol{H}_2$, which are the CTMs of BS-MS, BS-RS, and RS-MS links, respectively, the performance of direct transmission (DT), AF and DF relaying schemes is investigated. It is not fair to compare the channel capacity at the premise that all channel realizations are normalized to have the same channel gain [21, 22]. In our analysis, the effect of large scale fading is preserved. The power of CTMs with distance of r to the Tx is normalized according to the path loss (PL), i.e.,

$$\mathcal{E}\left\{\frac{\|\boldsymbol{H}(r)\|_F^2}{N_{\mathrm{Rx}}N_{\mathrm{Tx}}}\right\} = \frac{1}{PL(r)}. \tag{11}$$

The PL in dB was calculated as

$$PL_{dB}(r) = a + 10n \cdot \log_{10}(r), \tag{12}$$

where a is the intercept at 1 m, n is the path loss exponent, and r is the distance between Tx and Rx in meter. a and n are selected according to our previous measurement results [23] and standardization reports [24–27]. Table 5 lists the intercept a and path loss exponent n for different links.

A time domain duplex relay protocol is chosen for comparison among different transmission schemes. In order to complete the data transmission, two consecutive time slots are required in the protocol. In the first time slot, the BS broadcasts signals to the RS and MS. Afterwards, the RS communicates with the MS in the second time slot. For a fair comparison, the transmitting power of BS and RS, i.e., P_{BS} and P_{RS}, are allocated under the constraint that $P_{\mathrm{BS}} + P_{\mathrm{RS}} = P_0$. In our analysis, equal power allocation is assumed, namely $P_{\mathrm{BS}} = P_{\mathrm{RS}} = P_0/2$. The DT is considered as a baseline for comparison. Since only one time slot is required in the DT, the BS can use the first and second time slot to transmit different data with the transmitted power $P_0/2$. Assuming the thermal noises at all Rx have equal variance σ_n^2,

Table 4 Gaussian fitting results for BS-MS link and RS-MS link

	BS-MS		RS-MS	
	μ	σ	μ	σ
XPD_V LOS	4.4	8.1	2.9	8.4
XPD_H LOS	5.1	8.5	2.2	8.4
XPD_V NLOS	6.8	8.4	7.6	7.9
XPD_H NLOS	2.5	8.3	1.2	8.3

Table 5 Intercept a and path loss exponent n for different links

	BS-RS	BS-MS		RS-MS	
	LOS	LOS	NLOS	LOS	NLOS
a	11.7	28.0	22.7	41.7	32.9
n	3.76	2.80	2.67	2.09	3.75

Table 6 The SNR at Rx γ (dB) for different links

	BS-RS	BS-MS		RS-MS	
	LOS	LOS	NLOS	LOS	NLOS
γ	30	10–40	−10–15	10–35	−10–15

the SNR ρ is given by $\rho = P_0/2\sigma_n^2$. The SNR at Rx γ can be obtained as $\gamma = \rho\|\boldsymbol{H}\|_F^2$. Given P_0, the γ is variable. A fixed P_0 is selected, and the resulting γ values for different links are listed in Table 6.

5.1 Direct transmission

The channel capacity of the DT can be calculated as

$$C^{\mathrm{DT}} = \frac{1}{B}\int_B \log_2\det\left(\boldsymbol{I} + \frac{\rho}{N_{\mathrm{Tx}}}\boldsymbol{H}_0(t,f)\boldsymbol{H}_0^{\mathrm{H}}(t,f)\right)\mathrm{d}f, \tag{13}$$

where B is the bandwidth and N_{Tx} is number of Tx antennas [28]. For the discrete channel $\boldsymbol{H}(j,k)$, an approximation can be given by

$$C^{\mathrm{DT}}(j) \approx \frac{1}{K}\sum_{k=1}^{K}\log_2\det\left(\boldsymbol{I} + \frac{\rho}{N_{\mathrm{Tx}}}\boldsymbol{H}_0(j,k)\boldsymbol{H}_0^{\mathrm{H}}(j,k)\right). \tag{14}$$

For simplicity, the transmitted power is assumed to be allocated equally over all the antennas.

5.2 AF relaying scheme

In AF relaying mode, the RS amplifies the received signal from the BS and transmits it to the MS in the next time slot. To ensure that the total transmitted power in two time slots is restricted to P_0, the amplification factor g at the RS is selected as

$$g = \sqrt{\frac{P_0}{\frac{P_0}{N_{\mathrm{BS}}}\|\boldsymbol{H}_1\|_F^2 + 2N_{\mathrm{RS}}\sigma_n^2}}, \tag{15}$$

where g is the diagonal element of the amplification matrix $\boldsymbol{G}$. Given the amplification matrix $\boldsymbol{G}$, the capacity of kth frequency bin in AF relaying scheme can be obtained as below [29]:

$$C_k^{\mathrm{AF}} = \log_2\det\left(\boldsymbol{I} + \frac{P_0}{2N_{\mathrm{BS}}\sigma_n^2}\boldsymbol{H}_2\boldsymbol{G}\boldsymbol{H}_1\boldsymbol{H}_1^{\mathrm{H}}\boldsymbol{G}^{\mathrm{H}}\boldsymbol{H}_2^{\mathrm{H}} \times (\boldsymbol{I} + \boldsymbol{H}_2\boldsymbol{G}\boldsymbol{G}^{\mathrm{H}}\boldsymbol{H}_2^{\mathrm{H}})^{-1}\right). \tag{16}$$

Then, the C^{AF} can be obtained as

$$C^{\mathrm{AF}} = \frac{1}{2}\cdot\frac{1}{K}\sum_{k=1}^{K}C_k^{\mathrm{AF}}, \tag{17}$$

where the factor 1/2 is due to the half-duplex transmission.

5.3 DF relaying scheme

The RS retransmits the decoded signal to the MS after receiving signals from the BS in the previous time slot. The end-to-end system performance of DF relaying scheme is mainly dominated by characteristics of the link with worse performance, thus, the capacity can be obtained as

$$C^{\mathrm{DF}} = \frac{1}{2}\min\{C_1^{\mathrm{DF}}, C_2^{\mathrm{DF}}\}, \tag{18}$$

where C_1^{DF} and C_2^{DF} are the channel capacity of the BS-RS and RS-MS link, respectively. C_1^{DF} and C_2^{DF} can be calculated by substituting $\boldsymbol{H}_1$ and $\boldsymbol{H}_2$ into eq. (14).

The capacity of every routes for the DT, AF, and DF is calculated using eqs. (13), (16) and (17). The capacity results of different measurement spots with equal distance to the BS are averaged to characterize the whole measurement region. The capacity results of the DT, AF, and DF as a function of distance from BS are shown in Figure 4. For the LOS case, when the MS is near the BS (less than 150 m), the DT provides significantly higher capacity than the AF and DF. The result is caused by two factors. The first factor is the relative positions of BS, RS and MS. The distance between the BS and the MS is shorter than the distance between the RS and the MS (see Figure 1). The second is the LOS propagation between the BS and the MS. These two factors make it not necessary to utilize relay. When the MS moves beyond the distance of 150 m, the capacity curve of the DT manifests a steeper downward trend. When the MS reaches the distance of 200 m, the capacity of the DT drops to a similar level to the capacity of the DF. The results show that for the LOS propagation, especially when the MS is near the BS (routes 1 and 2 in Figure 1), the DT is the optimal scheme. It can also be found that the DF performs better than the AF, and the capacity difference is about 15 bits/s/Hz.

For the NLOS case, the DF outperforms the AF and DT for all the distances ranging from 30 to 250 m. Due to the NLOS propagation between the BS and the MS, even when the MS is close to the BS, the DF provides higher capacity than the DT. The capacity of the AF is similar to that of the DT, when the distance between the BS and the MS is less than 100 m. When the distance exceeds 100 m, the capacity of the DT becomes lower than that of the AF. The difference increases as the distance increases. The measurement results validate that the relay can provide higher capacity for users in the NLOS region of BS or users with relatively far distance from the BS.

5.4 Impact of antenna configuration

Three antenna configurations were employed at the RS to investigate the impact of the antenna on the capacity. The antenna configurations are illustrated in Figure 5. The first configuration consisted of four spatially separated antennas with same polarization ($+45°$). The second one used four spatially separated antennas with different polarizations ($+45°$ and $-45°$). Two pairs of dual-polarized ($\pm 45°$) antennas were utilized for the third configuration.

The capacity results of the AF and DF with different antenna configurations are given in Figure 6. From Figure 6(a), it can be found that for the LOS case, the second antenna configuration shows highest capacity. This is mainly because this configuration provide not only spatial diversity gain but also polarization diversity gain. By contrast, the first configuration, which only utilizes the spatial diversity gain, manifests the lowest capacity. The third configuration, which is in between the first and second configuration, provides the moderate capacity. For the NLOS case, these three configurations show similar capacity. The reasons are primarily as follows. In the NLOS scenario, XPD decreases (see Table 4), which reduces the polarization diversity gain. On the other hand, the NLOS propagation results in a larger angular spread, which produces a lower spatial correlation between antennas. As a consequence, the spatial diversity gain increases. Therefore, the capacity difference among three configurations almost disappears. From the comparison of Figures 6(a) and 6(b), we also observe that the antenna configuration has similar impact on the AF and DF schemes. The results reveal that the second antenna configuration, which provides both spatial and polarization diversity gain, is a robust antenna solution for all deployment conditions. The third configuration makes a compromise between equipment size and performance, and it is a good candidate when the equipment size is limited.

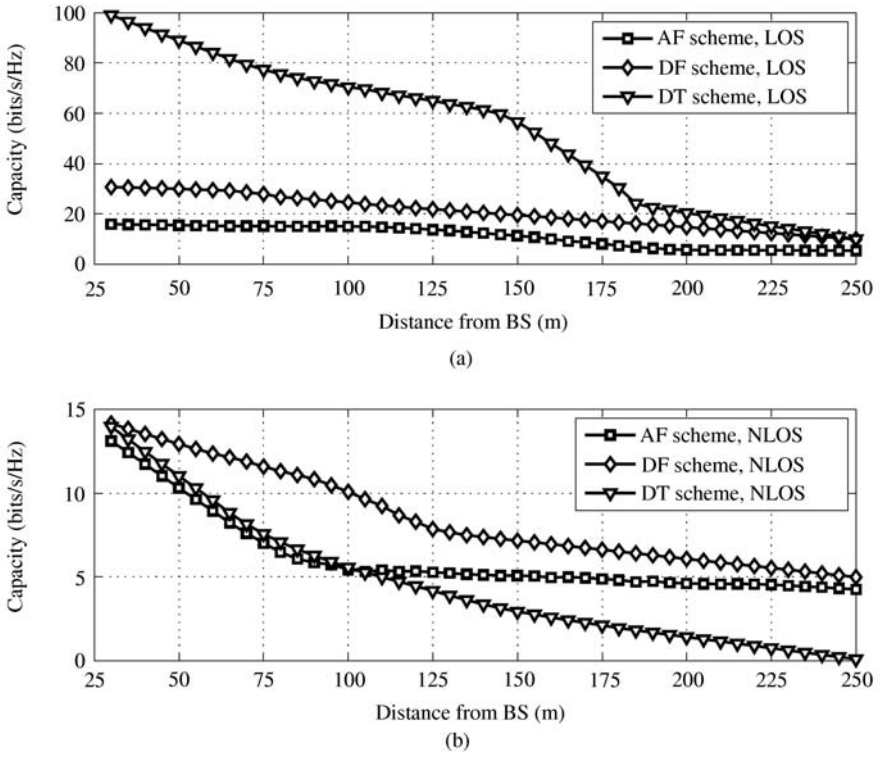

Figure 4 The capacity as a function of distance from BS for AF, DF, and DT schemes. (a) The capacity as a function of distance from BS for AF, DF, and DT schemes in LOS scenarios; (b) the capacity as a function of distance from BS from AF, DF, and DT schemes in NLOS scenarios.

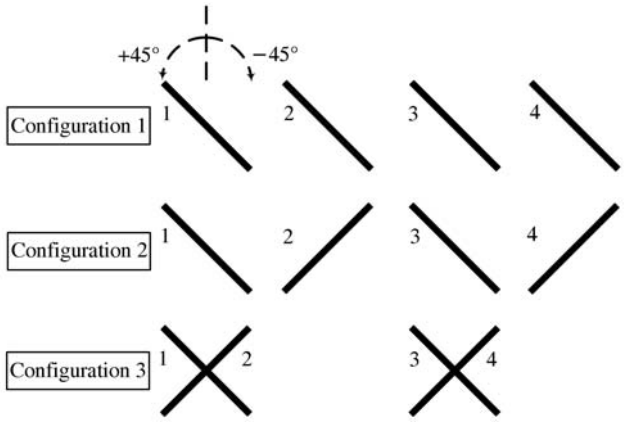

Figure 5 Different antenna configurations for RS.

6 Conclusions

In this paper, the potential of MIMO relay is investigated based on wideband outdoor measurements at 2.35 GHz in the outdoor urban scenario. To our knowledge, this measurement is the first MIMO relay measurement in China. Measurement and analysis results show that the relay provides better coverage for routes in the NLOS scenario of BS. With the combination of the DT, relay can provide better coverage for all routes in the measurement region. Due to difference in antenna height, three links manifest different characteristics. The BS-RS link is more static, and less power in different polarization is coupled. Scarce scatters around the BS lead to a smaller EDOF. In the BS-RS link, utilizing polarization diversity is more effective than spatial diversity. The XPD values of RS-MS link are smaller than those of the conventional BS-MS link. It is also found that the vertical polarization preserves better than horizontal polarization

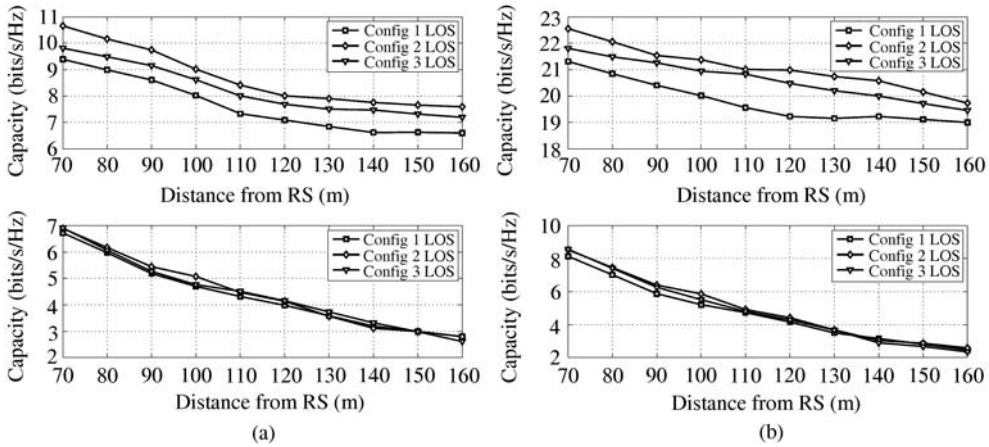

Figure 6 The capacity comparison of different RS antenna configurations. (a) The capacity for AF; (b) the capacity for DF.

in the NLOS scenario, especially in the RS-MS link. The EDOF of RS-MS link is larger than that of BS-MS link. Based on the measured CTMs, DT, AF and DF transmission schemes are assessed. In the case of the LOS propagation, especially when the MS is near the BS, the DT is the optimal scheme. The measurement results also validate that the relay can provide higher capacity for users in the NLOS region of BS or users with relatively far distance from the BS. Then, the performance of three antenna configurations for the RS is compared in terms of capacity. It is observed that spatially separated antennas with different polarizations provide the best performance, and polarization diversity is a robust MIMO solution under the constraint of equipment size. The measurement and analysis results can more accurately describe the propagation environment in the urban area of China, and provide more insights into the influence of the wireless channel on relay performance and relay deployment in urban scenario of China.

Acknowledgements

This work was supported in part by China Important National Science and Technology Specific Projects (Grant No. 2009ZX03007-003-01), the National High-Tech Research & Development Program of China (Grant No. 2009AA011502), and the National Natural Science Foundation of China (Grant No. 60772113).

References

1 Nosratinia A, Hunter T, Hedayat A. Cooperative communication in wireless networks. IEEE Commun Mag, 2004, 42: 74–80

2 Pabst R, Walke B, Schultz D, et al. Relay-based deployment concepts for wireless and mobile broadband radio. IEEE Commun Mag, 2004, 42: 80–89

3 Wang B, Zhang J, Host-Madsen A. On the capacity of MIMO relay channels. IEEE Trans Inf Theory, 2005, 51: 29–43

4 Yu M, Li J, Sadjadpour H. Amplify-forward and decode-forward: the impact of location and capacity contour. In: Proceedings of IEEE Military Communications Conference, Atlantic City, New Jersey, USA, 2005. 1609–1615

5 Laneman J, Wornell G, Tse D. An efficient protocol for realizing cooperative diversity in wireless networks. In: Proceedings of IEEE International Symposium on Information Theory, Washington, DC, USA, 2001. 294

6 Nabar R, Bolcskei H, Kneubuhler F. Fading relay channels: performance limits and space-time signal design. IEEE J Select Areas Commun, 2004, 22: 1099–1109

7 Kyritsi P, Eggers P, Gall R, et al. Measurement based investigation of cooperative relaying. In: VTC'06-Fall: Proceedings of IEEE 64th Vehicular Technology Conference, Montreal, Quebec, Canada, 2006. 1–5

8 Kyritsi P, Popovski P, Eggers P, et al. Cooperative transmission: a reality check using experimental data. In: VTC'07-Spring: Proceedings of IEEE 65th Vehicular Technology Conference, Dublin, Ireland, 2007. 2281–2285

9 Jiang L, Thiele L, Jungnickel V. Modeling and measurement of MIMO relay channels. In: VTC'08-Spring: Proceedings of IEEE 67th Vehicular Technology Conference, Singapore, 2008. 419–423

10 Haneda K, Kolmonen V M, Riihonen T, et al. Evaluation of relay transmission in outdoor-to-indoor propagation channels. In: Proceedings of COST2100 2nd Workshop on MIMO and Cooperative Communications, Valencia, Spain, 2008
11 Gao X Y, Zhang J H, Liu G Y, et al. Large-scale characteristics of 5.25-GHz based on wideband MIMO channel measurements. IEEE Antennas Wirel Propag Lett, 2007, 6: 263–266
12 Nie X, Zhang J H, Zhang Y, et al. An experimental investigation of wideband MIMO channel based on indoor hotspot NLOS measurements at 2.35-GHz. In: GLOBECOM'08: Proceedings of IEEE Global Telecommunications Conference, New Orleans, Louisiana, USA, 2008. 1–5
13 Herdin M. MIMO amplify-and-forward relaying in correlated MIMO channels. In: Proceedings of 15th International Conference on Information, Communications and Signal Processing, Bangkok, Thailand, 2005. 796–800
14 Pedersen T, Yin X F, Fleury B H. Estimation of MIMO channel capacity from phase-noise impaired measurements. In: GLOBECOM'08: Proceedings of IEEE Global Telecommunications Conference, New Orleans, Louisiana, USA, 2008. 1–6
15 Taparugssanagorn A, Ylitalo J, Fleury B H. Phase-noise in TDM-switched MIMO channel sounding and its impact on channel capacity estimation. In: GLOBECOM'07: Proceedings of IEEE Global Telecommunications Conference, Washington, DC, USA, 2007. 196–201
16 Taparugssanagorn A, Ylitalo J. Characteristics of short-term phase noise of MIMO channel sounding and its effect on capacity estimation. IEEE Trans Instrum Meas, 2009, 58: 196–201
17 Pedersen T, Taparugssanagorn A, Ylitalo J, et al. On the impact of TDM in estimation of MIMO channel capacity from phase-noise impaired measurements. In: Proceedings of IEEE International Zurich Seminar on Communications, Zurich, Switzerland, 2008. 128–131
18 Fleury B, Tschudin M, Heddergott R, et al. Channel parameter estimation in mobile radio environments using the SAGE algorithm. IEEE J Select Areas Commun, 1999, 17: 434–450
19 Shiu D S, Foschini G J, Gans M J, et al. Fading correlation and its effect on the capacity of multielement antenna systems. IEEE Trans Commun, 2000, 48: 502–513
20 Shafi M, Zhang M, Moustakas A, et al. Polarized MIMO channels in 3D: models, measurements and mutual information. IEEE J Select Areas Commun, 2006, 24: 514–527
21 Svantesson T, Wallace J. On signal strength and multipath richness in multi-input multi-output systems. In: ICC'03: Proceedings of IEEE International Conference on Communications, Anchorage, Alaska, USA, 2003. 2683–2687
22 Nishimoto H, Ogawa Y, Nishimura T, et al. Measurement based performance evaluation of MIMO spatial multiplexing in a multipath-rich indoor environment. IEEE Trans Antennas Propagat, 2007, 55: 3677–3689
23 Dong D, Zhang J H, Zhang Y, et al. Large scale characteristics and capacity evaluation of outdoor relay channels at 2.35-GHz. In: VTC'09-fall: Proceedings of IEEE 70th Vehicular Technology Conference, Anchorage, Alaska, USA, 2009
24 3GPP R1-091566. Relay to UE channel model for LTE-Advanced, 2009
25 3GPP R1-091567. Text Proposal for 36.814 on the Relay-to-UE channel model, 2009
26 3GPP TR 36.814 v0.4.1. Further Advancements for E-UTRA Physical Layer Aspects (Release 9), 2009
27 ITU-R M.2135. Guidelines for evaluation of radio interface technologies for IMT-Advanced, 2008
28 Paulraj A, Nabar R, Gore D. Introduction to Space-Time Wireless Communications. Cambridge: Cambridge University Press, 2003
29 Munoz O, Vidal J, Agustin A. Non-regenerative MIMO relaying with channel state information. In: ICASSP'05: Proceedings of IEEE International Conference on Acoustics, Speech, and Signal Processing, Philadelphia, Pennsylvania, USA, 2005. 361–364